

# Hierarchical Edge-Cloud Task Offloading in NTN for Remote Healthcare

Alejandro Flores\*; Danial Shafaie+, Konstantinos Ntontin\*, Elli Kartsakli+, Symeon Chatzinotas\*

\*Interdisciplinary Centre for Security, Reliability and Trust (SnT), University of Luxembourg, Luxembourg.

+Barcelona Supercomputing Center, Spain.

e-mails: \*{alejandro.flores, kostantinos.ntontin, symeon.chatzinotas}@uni.lu;

+{danial.shafaie, elli.kartsakli}@bsc.es

**Abstract**—In this work, we study a hierarchical non-terrestrial network as an edge-cloud platform for remote computing of tasks generated by remote ad-hoc healthcare facility deployments, or internet of medical things (IoMT) devices. We consider a high altitude platform station (HAPS) to provide local multiaccess edge server (MEC) services to a set of remote ground medical devices, and a low-earth orbit (LEO) satellite, serving as a bridge to a remote cloud computing server through a ground gateway (GW), providing a large amount of computing resources to the HAPS. In this hierarchical system, the HAPS and the cloud server charges the ground users and the HAPS for the use of the spectrum and the computing of their tasks respectively. Each tier seeks to maximize their own utility in a selfish manner. To encourage the prompt computation of the tasks, a local delay cost is assumed. We formulate the optimal per-task cost at each tier that influences the corresponding offloading policies, and find the corresponding optimal bandwidth allocation.

**Index Terms**—multi-access edge computing (MEC), non-terrestrial networks, resource allocation, task offloading, healthcare 4.0.

## I. INTRODUCTION

Healthcare 4.0 (H4.0) envisions the persistent data gathering, sharing and processing from patients to healthcare providers and healthcare entities, which enables enhanced treatment through remote monitoring, proactive treatment, disease prevention and intelligent disease treatment [1]. Biosignal data gathered from patients, through specialized healthcare sensors, or through internet of medical things (IoMT) devices enables making appropriate health-related inferences [2], [3]. These inferences are abstracted as computing tasks that can be processed locally, or offloaded to remote edge or cloud servers if the local resources are constrained, or if the results need to be allocated particularly promptly. In remote locations, disaster situations [4], or war zones [5], ad-hoc healthcare facilities can be deployed to provide healthcare services to people in need. However, due to the nature of these environments, a local ground cellular network may not be available due to their destruction, congestion, or remoteness of the area, given that only 15% of the surface of the Earth has cellular coverage [6].

As a solution to these problems, non-terrestrial networks (NTNs), which comprise air nodes such as high altitude platform stations (HAPS), and space nodes such as low-earth orbit (LEO) satellites, can act as multi-access edge servers (MEC) or bridges to remote mobile cloud computing (MCC) servers, to offload computing tasks generated by the ground healthcare

nodes. Connection to satellite constellations orbiting the Earth, in general belonging to different companies [7], is generally performed by acquiring the corresponding user terminal and subscription from the vendor. LEO satellites are typically resource-constrained and better suited to relay information to a remote cloud server within coverage [8]. HAPS may be deployed on a case-by-case basis to directed zones, being able to connect to arbitrary user terminals [9] and accommodate larger payloads, allowing greater computing capacity.

There is recent literature on the use of hybrid TN-NTNs for task offloading. In [10] we explored the non-orthogonal resource initialization of NTN MEC-enabled nodes for task offloading to a LEO satellite through intermediate UAVs. Hybrid MEC-enabled satellite networks have also been studied, such as in [11] via a two-level hierarchical game for edge–cloud collaboration and joint task offloading and resource allocation. Pricing and hierarchy also appear in [12] which studies a Stackelberg game in TN-NTN relaying and in robustness settings such as in [13]. Also, a complete model for selfish task offloading was studied in [14], introducing a Game theoretic modeling. Targeting the research gaps, our work studies remote healthcare applications in NTN with a three-tier non-collaborative computing infrastructure. Unlike prior studies that mainly optimize offloading and computing resource allocation, we derive the optimal bandwidth allocation scheme, while proposing a game theoretic solution for offloading decisions and setting prices, for healthcare-related data models.

## II. SYSTEM MODEL

Assume an ad-hoc healthcare deployment has been installed in a remote location, due to a general disaster situation. The healthcare ground devices (GDs), represented by the set  $\mathcal{I}$  do not have access to a terrestrial network due to the geographical remoteness. Each GD gathers biosignal-related data from the patients, and, at a given snapshot of the system, generates a computing task  $\psi_i = [d_i, \mu_i, \tau_i^{\max}]^T$  related to the data gathered, where  $d_i$  is the number of bits of the task,  $\mu_i$  is its computation density in CPU cycles per bit in Hz, and  $\tau_i^{\max}$  is the maximum delay allowed for its completion. A local HAPS  $h$  with MEC capabilities is deployed, which can compute tasks generated by the GDs, transmitted through a shared wireless channel of bandwidth  $B_u$ . The HAPS charges

the GDs a price  $c_{B_u}$  per unit bandwidth to access the wireless channel in the S band, and a price  $c_i^{\text{MEC}}$  to compute their corresponding tasks. Furthermore, the HAPS can connect to LEO satellite  $s$  belonging to a different provider, through a wireless channel of bandwidth  $B_h$  in the Ka band. The LEO satellite acts as a bridge to a remote MCC server, through a ground gateway  $g$ , which offers ample computing capabilities. We assume the HAPS does not have access to the terrestrial infrastructure given the remoteness of the location, thus, the satellite system charges the HAPS a price of  $c_{B_h}$  per unit bandwidth to access the wireless channel, and a price  $c_i^{\text{MCC}}$  to compute the corresponding task  $\psi_i$ . Figure 1 shows the system model considered.

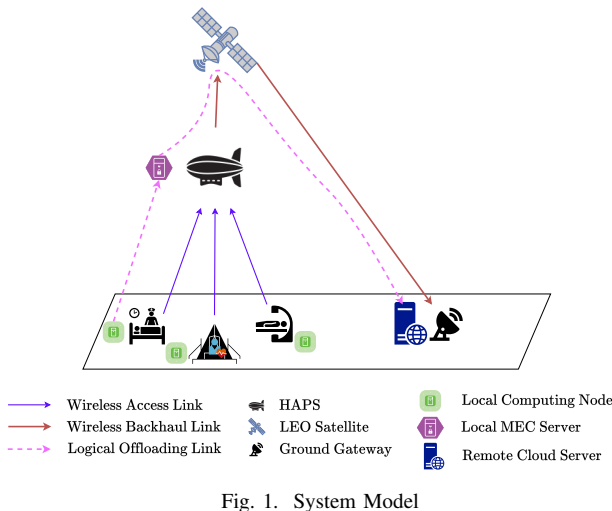


Fig. 1. System Model

#### A. Channel Model

The HAPS has a uniform planar array (UPA) of  $M_h^d$  antenna elements for GD access, and a UPA of  $M_h^u$  antenna elements for access to the LEO satellite. The LEO satellite and the GW have UPAs of  $M_s$  and  $M_g$  antenna elements respectively. The IoMT-HAPS channels  $\mathbf{h}_{i,h}$  includes an air-to-ground pathloss component given as in [15], and a Rician small-scale fading component modeled as in [16]. To receive the signals sent by the GDs, the HAPS employs a maximum-ratio combiner, having a channel gain of  $g_{i,h} = \|\mathbf{h}_{i,h}\|^2$ .

The links between the HAPS and the LEO satellite, and between the LEO satellite and the GW are orthogonal of bandwidth  $B_h$ . Given the spatial sparsity of the links, we assume LoS-MIMO channels, for which the corresponding channel gains are given as  $g_{j,k} = M_j M_k \left( \frac{\lambda_k G_{u,k}}{4\pi \|\mathbf{r}_j - \mathbf{r}_k\|_2} \right)^2$ , with  $j \in \{h, s\}$ ,  $k \in \{s, g\}$ ,  $G_{u,k}$  includes the atmospheric losses due to weather phenomena, and  $\lambda_k$  is the corresponding wavelength. Then, the communication rate between node  $j \in \mathcal{I} \cup \{h, s\}$  and  $k \in \{h, s, g\}$  is

$$R_{j,k} = \rho_j B_{j \rightarrow k} \log_2 \left( 1 + \frac{g_{j,k} p_j}{\rho_j B_k N_0} \right), \quad (1)$$

where  $\rho_j$  is the proportion of the bandwidth available used by node  $j$ ,  $B_{j \rightarrow k} \in \{B_u, B_h\}$  is the total bandwidth available for

the link,  $N_0$  is the noise power per unit bandwidth at reception, and  $p_j$  is the corresponding transmit power.

#### B. Delay Model

1) *Transmission Delay*: The transmission delay experienced by offloading task  $\psi_i$  from GD  $i$  to the HAPS  $h$  is given as  $\tau_{i,h} = \frac{d_i}{R_{i,h}}$ . In the delay experienced by offloading the corresponding tasks from  $j \in \{h, s\}$  to  $k \in \{s, g\}$  the round-trip propagation delay cannot be neglected, due to the large distances, and is given as  $\tau_{j,k} = \frac{1}{R_{j,k}} \sum_{i \in \mathcal{I}_h} \beta_{h,s}^i d_i + 2\tau_{j,k}^{\text{prop}}$ , where  $\tau_{j,k}^{\text{prop}} = \frac{1}{c} \|\mathbf{r}_j - \mathbf{r}_k\|_2$ . The offloading decision variable  $\beta_{h,s}^i = 1$  if task  $\psi_i$  is offloaded from  $h$  to  $s$  and  $\beta_{h,s}^i = 0$  otherwise. Likewise,  $\beta_{u,h}^i = 1$  if task  $\psi_i$  is offloaded from GD  $i$  to  $s$  and  $\beta_{u,h}^i = 0$  otherwise.

2) *Computing Delay*: Task  $\psi_i$  can be computed locally at GD  $i \in \mathcal{I}$ , or remotely at the HAPS or the remote MCC. If node  $k \in \mathcal{I} \cup \{h\}$  computes the task, the computing delay is  $\tau_i^k = \frac{d_i \mu_i}{f_i^k}$ , where  $f_i^k$  are the resources allocated for the task by node  $k$ . If it is computed at the MCC, the processing delay is assumed as negligible, due to its vast computing resources.

#### C. Cost Model

The cost of computing or offloading a task is defined by the cost of bandwidth, the cost of remote computing and a delay cost to incentivize its prompt execution.

1) *Cost for GDs*: We suppose a virtual cost of  $c_\tau$  per second spent in computing the task; that the ground devices pay  $c_{B_u}$  per Hz of the use of the spectrum to the HAPS; and that the MEC server sets and advertises a cost  $c_i^{\text{MEC}}$  for computing the task. Thus, cost for GD  $i$  is

$$C_i^{\text{loc}} = (1 - \beta_{u,h}^i) c_\tau \tau_i^i + \beta_{u,h}^i (c_\tau \tau_{i,h} + c_{B_u} \rho_i B_u + c_i^{\text{MEC}}). \quad (2)$$

2) *Cost and Utility for MEC server*: The MEC server earns a profit from the offloading of a task from GD  $i$ . If it offloads it to the MCC through the LEO satellite, it incurs a processing cost and bandwidth cost. The LEO charges the HAPS  $c_{B_h}$  per Hz of the use of the spectrum. Thus, the total cost incurred by the HAPS is

$$C^{\text{MEC}} = c_{B_h} \rho_B B_h - \sum_{i \in \mathcal{I}} \beta_{u,h}^i (c_{B_h} \rho_i B_u + c_i^{\text{MEC}}) \quad (3)$$

$$+ \sum_{i \in \mathcal{I}} (\beta_{u,h}^i - \beta_{h,s}^i) c_\tau \tau_i^h + \sum_{i \in \mathcal{I}} \beta_{h,s}^i (c_\tau (\tau_{h,s} + \tau_{s,g}) + c_i^{\text{MCC}}).$$

3) *Utility for Cloud Server*: The cloud server benefits from the computing of its tasks as

$$C^{\text{MCC}} = -c_{B_h} \rho_B B_h - \sum_{i \in \mathcal{I}} \beta_{h,s}^i c_i^{\text{MCC}} \quad (4)$$

### III. PROBLEM FORMULATION

Each entity in the system seeks to maximize its utility. The satellite system computes the optimal cost per task to the HAPS, represented by the following optimization problem:

$$\mathcal{P}^{\text{MCC}} : \min_{\{c_i^{\text{MCC}}\}} C^{\text{MCC}} \quad (5a)$$

$$\text{s.t.} \quad C_1^c : c_i^{\text{MCC}} \geq 0 \quad (5b)$$

The HAPS computes the optimal offloading strategy to the cloud and the corresponding share of the bandwidth, as well as the optimal cost per task to each GD that solves the following optimization problem

$$\mathcal{P}^{\text{MEC}} : \min_{\substack{\{c_i^{\text{MEC}}\} \\ \{\beta_{u,s}^i\}, \rho_B}} C^{\text{MEC}} \quad (6a)$$

$$C_1^m : \tau_{i,h} + \left(1 - \beta_{u,s}^i\right) \tau_i^h \quad (6b)$$

$$+ \beta_{u,s}^i (\tau_{h,s} + \tau_{s,g}) \leq \tau_i^{\max} \quad \forall i \in \mathcal{I}$$

$$C_2^m : \beta_{h,s}^i \in \{0, 1\}, \quad \forall i \in \mathcal{I} \quad (6c)$$

$$C_3^m : 0 \leq \rho_B \leq 1. \quad (6d)$$

$$C_4^m : c_i^{\text{MEC}} \geq 0. \quad \forall i \in \mathcal{I} \quad (6e)$$

where  $C_1^m$  enforces the maximum delay constraint,  $C_2^m$  indicates that the offloading decisions are binary,  $C_3^m$  indicates that a non-negative proportion of the bandwidth to the MCC is used, and  $C_4^m$  indicates that costs are non-negative.

Each GD  $i \in \mathcal{I}$  maximizes its own utility, by determining their offloading strategy and portion of the bandwidth, that solves the following optimization problem

$$\mathcal{P}_i^{\text{loc}} : \min_{\substack{\beta_{u,h}^i, \rho_i}} C_i^{\text{loc}} \quad (7a)$$

$$C_1^l : \left(1 - \beta_{u,h}^i\right) \tau_i^i + \beta_{u,h}^i \left(\tau_{i,h} + \tau_i^h\right) \leq \tau_i^{\max} \quad (7b)$$

$$C_2^l : \beta_{u,h}^i \in \{0, 1\}, \quad (7c)$$

$$C_3^l : \rho_i + \sum_{j \in \mathcal{I}, j \neq i} \rho_j \leq 1 \quad (7d)$$

$$C_4^l : 0 \leq \rho_i \leq 1, \quad (7e)$$

where  $C_1^l$  indicates the maximum delay constraint of the task, and considers only offloading to the HAPS, without information of the space segment.  $C_2^l$  indicates that the offloading is binary,  $C_3^l$  limits the total bandwidth of the channel to the HAPS across GDs, and  $C_4^l$  indicates that a non-negative proportion of the bandwidth to the HAPS is used.

#### IV. PROPOSED SOLUTION

In IV-A we propose selfish price-setting policies for offloading, whereas in IV-B we derive the optimal spectrum allocation.

##### A. Price Setting and Offloading

Solving  $\mathcal{P}^{\text{MCC}}$  and  $\mathcal{P}^{\text{MEC}}$  in isolation will cause the prices to go to infinity, minimizing their cost. However, the inherent competition over utility prevents the parties from doing so. To capture this, we model this scenario as a competition between tiers, and develop a game-theoretic framework to solve it, where the cost and offloading problems are solved simultaneously. The players are the three tiers with computation capabilities. To separate the interactions, we decompose (3). The corresponding partial cost for the interaction between GD and MEC is given as  $C^{\text{MEC,loc}} = \sum_{i \in \mathcal{I}} \beta_{u,h}^i (c_\tau \tau_i^h - c_B \rho_i B_u - c_i^{\text{MEC}})$ . Likewise, the partial cost corresponding to the interaction between the HAPS and the MCC is given as  $C^{\text{MEC,MCC}} = c_{B_h} \rho_B B_h +$

$\sum_{i \in \mathcal{I}} \beta_{h,s}^i (c_\tau (\tau_{h,s} + \tau_{s,g} - \tau_i^h) + c_i^{\text{MCC}})$ . The interactions are analyzed in an extensive-form game.

Considering (2), (4),  $C^{\text{MEC,loc}}$  and  $C^{\text{MEC,MCC}}$ , it can be seen that GD has control over offloading and the MCC over pricing policy, whereas the HAPS can decide over the two policies: offloading to the MCC, pricing to the GDs. As the first round of policy setting, the MCC sets its strategy knowing the response from HAPS, which is modeled as:

$$\min_{\{c_i^{\text{MCC}}\}} C^{\text{MCC}} \quad (8)$$

The MCC reports the chosen price to the HAPS, which then sets the corresponding offloading variables  $\beta_{h,s}^i$  with fixed bandwidth allocation as

$$\begin{aligned} \min_{\{\beta_{h,s}^i\}} & C^{\text{MEC,MCC}} (c_i^{\text{MCC}}) \\ \text{s.t. } & \beta_{h,s}^i \in \{0, 1\}, \quad \forall i \in \mathcal{I} \end{aligned} \quad (9)$$

The feasibility constraints will be enforced on the solution of the game theoretic framework. Using backward induction, as the MCC knows the following action from the HAPS, it will set its policies accordingly.

The interaction between HAPS and the GDs is modelled by the following problem

$$\min_{\{c_i^{\text{MEC}}\}} C^{\text{MEC,loc}} \quad (10)$$

Following the resulting policy, the GDs determine the offloading strategy as

$$\begin{aligned} \min_{\{\beta_{u,h}^i\}} & C_i^{\text{loc}} (c_i^{\text{MEC}}) \\ \text{s.t. } & \beta_{u,h}^i \in \{0, 1\}, \quad \forall i \in \mathcal{I} \end{aligned} \quad (11)$$

As the equations are affine with respect to the values of  $\beta$  at different tiers, the optimization will yield a marginal value. As for the price policies, players will try to minimize their cost, setting the boundary values where offloading is not interrupted. A further bound is derived by considering the maximum delay constraint. Considering the game theoretic solution of (8) (9) we have

$$\bar{c}_i^{\text{MCC}} < c_\tau [\tau_i^h - \tau_{h,s} - \tau_{s,g}]^+ \quad (12)$$

Adding the delay constraint (6b) we have

$$\bar{c}_i^{\text{MCC}} \leq c_\tau (\tau_i^{\max} + \tau_i^h - 2\tau_{h,s} - 2\tau_{s,g} - \tau_{i,h}) \quad (13)$$

Thus, the price policy is given as

$$\hat{c}_i^{\text{MCC}} = \min\{\bar{c}_i^{\text{MCC}}, \bar{c}_i^{\text{MEC}}\} \quad (14)$$

For the second game, a similar approach is followed, considering equations (10), (11) and (7b)

$$\hat{c}_i^{\text{MEC}} < [c_\tau \tau_i^i - c_\tau \tau_{i,h} - c_B \rho_i B_u]^+ \quad (15)$$

$$\hat{c}_i^{\text{MEC}} \leq c_\tau (\tau_i^i - \tau_i^h - 2\tau_{i,h} + \tau_i^{\max}) - c_B \rho_i B_u \quad (16)$$

Forming the final policy as

$$\bar{c}_i^{\text{MEC}} = \min\{\hat{c}_i^{\text{MEC}}, \bar{c}_i^{\text{MEC}}\} \quad (17)$$

It is worth noting that the delay constraint ensures service provision, even at the cost of higher expenses for the players.

## B. Spectrum Allocation

1) *HAPS-GW*: Let  $\mathcal{I}^s$  be the set of tasks offloaded from the HAPS to the MCC. We assume a constant transmit power per unit bandwidth from the HAPS and the LEO satellite  $\hat{p}_{i,k} = \frac{p_{i,k}}{\rho_B B_h}$ . Then, after some algebraic manipulation we can write (3) as a function of  $\rho_B$  as  $C_i^{\text{MEC}} = \frac{a_h}{\rho_B} + b_h \rho_B$  where

$$a_h = \frac{c_\tau I^s \sum_{i \in \mathcal{I}^s} d_i}{B_h} \left( \frac{1}{\log_2 \left( 1 + \frac{g_{h,s} \hat{p}_{h,s}}{N_0} \right)} + \frac{1}{\log_2 \left( 1 + \frac{g_{s,g} \hat{p}_{s,g}}{N_0} \right)} \right) \quad (18)$$

$$b_h = c_{B_h} B_h \quad (19)$$

which is a convex function over  $\rho_B > 0$ . By taking its first derivative and equaling it to zero, its optimal point is given at  $\rho_B^{\text{opt}} = \sqrt{\frac{a_h}{b_h}}$ . Furthermore, to ensure that constraint  $C_1^m$  is met, it must hold that

$$\rho_B \geq \underbrace{\frac{a_h}{c_\tau I^s \min_{i \in \mathcal{I}^s} \left\{ \tau_i^{\max} - \left( \tau_{i,h} + 2 \left( \tau_{h,s}^{\text{prop}} + \tau_{s,g}^{\text{prop}} \right) \right) \right\}}}_{\rho_{B,1}^{\min}} \quad (20)$$

To ensure that the cost for offloading does not go above the cost of local execution, it needs to hold that

$$\frac{a_h}{\rho_B} + b_h \rho_B \leq \underbrace{\sum_{i \in \mathcal{I}^s} (c_\tau \tau_i^h - c_i^{\text{MCC}})}_{\sigma} \quad (21)$$

This expression can be converted into the quadratic convex form  $b_h \rho_B^2 - \sigma \rho_B + a_h \leq 0$ . By finding the cuts to zero of the function, we can convert this into the following equivalent linear constraint

$$\underbrace{\frac{\sigma - \sqrt{\sigma^2 - 4b_h a_h}}{2b_h}}_{\rho_{B,2}^{\min}} \leq \rho_B \leq \underbrace{\frac{\sigma + \sqrt{\sigma^2 - 4b_h a_h}}{2b_h}}_{\rho_B^{\max}} \quad (22)$$

which implies that  $\sigma \geq 2\sqrt{b_h a_h}$  must hold. We set  $\rho_B^{\min} = \max\{\rho_{B,1}^{\min}, \rho_{B,2}^{\min}\}$ . Then, the bandwidth allocation algorithm for the HAPS-LEO-GW is given as in Algorithm 1.

---

### Algorithm 1: HAPS-LEO-GW Bandwidth allocation

---

```

1 repeat
2   | Set  $\beta_{h,s}^{i^*} = 0$  for  $i^* = \text{argmin} \{c_\tau \tau_i^h - c_i^{\text{MCC}}\}$ ;;
3 until  $\sigma \geq 2\sqrt{b_h a_h}$ ;
4 repeat
5   | Set  $\beta_{h,s}^{i^*} = 0$  for  $i^* = \text{argmin} \{\tau_i^{\max} - \tau_{i,h}\}$ ;;
6 until  $\rho_B^{\min} \leq 1$  and  $\rho_B^{\min} \leq \rho_B^{\max}$ ;;
7 if  $\rho_B^{\min} \leq \rho_B^* \leq \rho_B^{\max}$  then
8   | Set  $\rho_B = \rho_B^*$ ;;
9 else
10  | Set  $\rho_B = \text{argmin} \{C_i^{\text{MEC}}(\rho_B^{\min}), C_i^{\text{MEC}}(\rho_B^{\max})\}$ ;;

```

---

2) *GD-HAPS*: Let  $\mathcal{I}^h$  be the set of tasks offloaded from the GDs to the HAPS. Similar to the HAPS-GW link, the optimal solution of the objective function for GD  $i \in \mathcal{I}^h$  is given as  $\rho_i^* = \sqrt{\frac{a_i}{b_i}}$ , where

$$a_i = \frac{c_\tau d_i}{B_u \log_2 \left( 1 + \frac{g_{i,h} \hat{p}_{i,k}}{N_0} \right)} \quad (23)$$

$$b_i = c_B B_u \quad (24)$$

This solution is generally not jointly feasible for all GDs, as  $C_2^l$  is not generally met. If the total amount of spectral resources are fully occupied, and the local optimal for a given GD is not met, requesting more spectral resources would increase the cost of the other GDs. This is a Pareto-optimal point. Thus, we find the solution as a fair Pareto-optimal point with the following min-max optimization problem:

$$\mathcal{P}_R^{\text{loc}} : \min_{\{\rho_i\}} \max_{i \in \mathcal{I}^h} C_i^{\text{loc}} \quad (25a)$$

$$C_1^L : \rho_i \geq \frac{a_i}{c_\tau (\tau_i^{\max} - \tau_i^h)} = \rho_{i,1}^{\min} \quad (25b)$$

$$C_2^L : \sum_{i \in \mathcal{I}^h} \rho_i \leq 1 \quad (25c)$$

$$C_3^L : 0 \leq \rho_i \leq 1 \quad \forall i \in \mathcal{I}^h \quad (25d)$$

$$C_4^L : c_\tau \tau_{i,h} + c_B \rho_i B_u + c_i^{\text{MEC}} \leq c_\tau \tau_i^h \quad \forall i \in \mathcal{I}^h \quad (25e)$$

Constraint  $C_4^L$  is needed so that tasks offloaded are only the ones that benefit from non-local computing, and can be written as  $\frac{a_i}{\rho_i} + b_i \rho_i \leq c_\tau \tau_i^h - c_i^{\text{MEC}}$ . The problem can be written in epigraph form as

$$\mathcal{P}^{\text{loc}} : \min_{\{\rho_i\}, \eta} \eta \quad (26a)$$

$$C_1^{LE} : \frac{a_i}{\rho_i} + b_i \rho_i \leq \eta \quad \forall i \in \mathcal{I}^h \quad (26b)$$

$$C_1^L, C_2^L, C_3^L, C_4^L \quad (26c)$$

Constraint  $C_4^L$  can be disregarded by ensuring  $\eta \leq \min_{i \in \mathcal{I}^h} \{c_\tau \tau_i^h - c_i^{\text{MEC}}\} = \eta^{\max}$ . Furthermore, similar to the previous section, constraint  $C_1^{LE}$  can be written as

$$\underbrace{\frac{\eta - \sqrt{\eta^2 - 4b_i a_i}}{2b_i}}_{\rho_{i,2}^{\min}} \leq \rho_i \leq \underbrace{\frac{\eta + \sqrt{\eta^2 - 4b_i a_i}}{2b_i}}_{\rho_i^{\max}} \quad (27)$$

which implies the constraint  $\eta \geq 2 \max_{i \in \mathcal{I}^h} \{\sqrt{b_i a_i}\} = \eta^{\min}$ .

We set  $\rho_i^{\min} = \max\{\rho_{i,1}^{\min}, \rho_{i,2}^{\min}\}$ . With this in mind, we can define a bisection-based algorithm to find the appropriate  $\eta$  value values, which runs for a set number of iterations  $N_\nu$ , and guarantees convergence within a precision of  $\varepsilon = 2^{-N_\nu} (\eta^{\max} - \eta^{\min})$ . From this the optimal  $\rho_i$  values can be found. The GD-HAPS bandwidth allocation algorithm is presented in Algorithm 2.

## V. RESULTS

### A. Communication Parameters

The carrier frequency for the HAPS-LEO link is in the Ka band, chosen as 28GHz, with bandwidth  $B_h = 100\text{MHz}$  [17].

**Algorithm 2:** GD-HAPS Bandwidth allocation

---

```

1 repeat
2   | Set  $\beta_{u,h}^{i^*} = 0$  for  $i^* = \operatorname{argmin} \{\tau_i^{\max} - \tau_i^h\}$ ;;
3   until  $\sum_{i \in \mathcal{I}^h} \rho_{i,1}^{\min} \leq 1$ ;;
4 repeat
5   | Set  $\beta_{u,h}^{i^*} = 0$  for  $i^* = \operatorname{argmin} \{c_\tau \tau_i^h - c_i^{\text{MEC}}\}$ ;;
6   until  $\sum_{i \in \mathcal{I}^h} \rho_{i,2}^{\min} (\eta^{\max}) \leq 1$  and  $\eta^{\min} \leq \eta^{\max}$ ;;
7 Find  $\eta^*$  through bisection between  $\eta^{\min} \leq \eta \leq \eta^{\max}$  such
  that

$$\sum_{i \in \mathcal{I}^h} \max \left\{ \frac{\eta - \sqrt{\eta^2 - 4b_i a_i}}{2b_i}, \frac{a_i}{c_\tau (\tau_i^{\max} - \tau_i^h)} \right\} \leq 1$$

  ;
8 For all  $i \in \mathcal{I}^h$  if  $\rho_i^{\min} \leq \rho_i^* \leq \rho_i^{\max}$  then
9   | Set  $\rho_i = \rho_i^*$ ;;
10 else
11   | Set  $\rho_i = \operatorname{argmin} \{C_i^{\text{loc}}(\rho_i^{\min}), C_i^{\text{loc}}(\rho_i^{\max})\}$ 

```

---

For the IoT-HAPS access, we assume LTE-M enabled IoMT devices working in LTE channel [18], we choose a subchannel bandwidth of  $B_u = 1.4\text{MHz}$ , accommodating  $|\mathcal{I}| = 14$  GDs per snapshot, over the carrier at 2.1GHz. The nodes are located around the center of coordinates, while the HAPS, LEO satellite and gateway are located at  $\mathbf{r}_h = [0, 0, 20]\text{km}$ ,  $\mathbf{r}_s = [0, 5, 500]\text{km}$ , and  $\mathbf{r}_g = [0, 10, 0]\text{km}$  respectively. We consider the MEC at the HAPS has  $F_h = 10\text{GHz}$  of computing resources, and transmit powers of  $p_i = 500\text{mW}$ ,  $p_h = 2\text{W}$  and  $p_s = 1\text{W}$ , over their total correspondent bandwidth of  $B_u = 20\text{MHz}$  and  $B_h = 200\text{MHz}$ . For comparison, we set the bandwidth cost as  $c_{B_u} = c_{B_h} = 1 \times 10^{-13}$ .

### B. Healthcare Task Model

We consider three types of healthcare-related data

- Large payload medical data, such as echocardiogram data, as 640x480 pixels images, with 8 bits per pixel, acquired at 1Hz, and utilizing 3:1 lossless compression [19], resulting in a generation of data at the rate of 819.2 Kbps.
- Medium payload medical data, such as electrocardiogram (ECG) data generated at 500 Hz from 12 leads, represented in 32 bits each [20], generating data at 192 Kbps rate.
- Low payload medical data, such as photoplethysmography (PPG) data from wearable devices, generated at 64 Hz in single-precision doubles [21], generating data at 2.048 Kbps.

For comparison, we take uniform time intervals for data offloading of 100 ms over a 1 Mbps data rate, which results in packets of approximately 82 Kbs, 20 Kbs and 200 bits respectively. Moreover, to account for variations in the data gathering of the devices and decisions to offload certain samples or not, we consider that the size of the tasks follow normal distributions around those values. Furthermore, we consider a high computing density of  $\mu_i = 500$  cycles per bit for the large payload data, and a small computing density of  $\mu_i = 50$  cycles per bit for the medium and low payload

data. Moreover, we choose maximum delays constraints of  $\tau_i^{\max} \in \{500, 50, 1\}$  ms for the large, medium, and low payload data, respectively.

### C. Performance Evaluation

We compare the results of our proposed solution to a benchmark of fixed cost for all tasks, set as the highest cost obtained across all of them, and a benchmark of a solution without bandwidth optimization. We

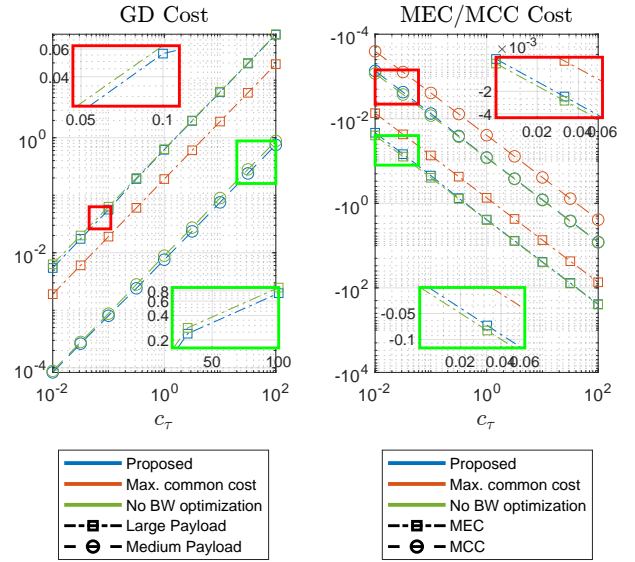


Fig. 2. Per-tier cost over virtual delay cost  $c_\tau$ .

In Fig 2, we show the real cost (without the virtual delay cost) obtained by the GDs, the MEC and the MCC. Note that negative costs imply utility. As  $c_\tau$  increases, the tasks are further incentivized to be offloaded to servers with higher capacity for faster computing of their tasks, thus the MEC and MCC can charge more for task computing. Nevertheless, this is only mostly true for the larger payload tasks, as low-payload tasks are computed locally with smaller delay than transmitting them. Furthermore, fixing the maximum cost dis-incentivizes offloading, reducing the utility at the MEC/MCC and the cost at the GDs, at the expense of faster task executions. On the other hand, not including the bandwidth optimization has the largest impact for smaller  $c_\tau$  values, where it reduces the cost at the GDs at the expense of also reducing utility at the MEC/MCC.

In Fig 3 we show the location where tasks belonging to each of the three task types are computed. There is a clear tendency where higher-load tasks are computed at larger-resource nodes, where large payload tasks tend to be computed at the MCC, medium payload tasks tend to be computed at the HAPS MEC, and low payload tasks tend to be computed locally. Moreover, the proposed solution controls for remote infeasibilities and large costs in the bandwidth allocation problem, which causes more medium and large payload tasks to be computed locally, which prevents the remote servers from causing infeasibilities. Furthermore, the max. common cost benchmark is the one

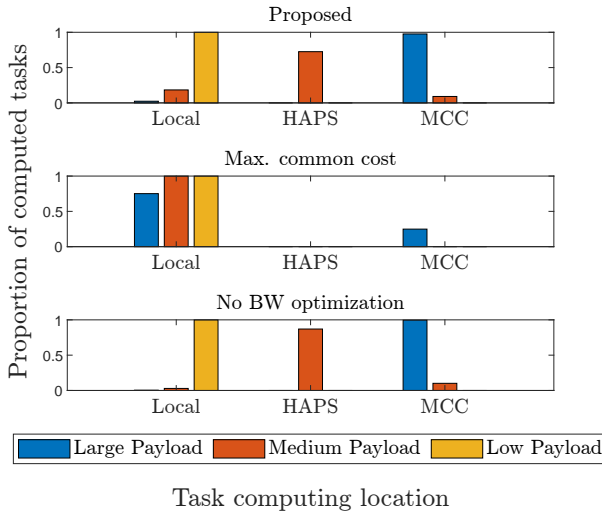


Fig. 3. Computing location of tasks per task type.

where the least amount of tasks are offloaded, due to the large costs for remote task processing.

## VI. CONCLUSIONS

We studied a hierarchical NTN edge-cloud task offloading architecture where each tier incurs costs when offloading tasks to a higher layer, while gaining profit from the tasks offloaded to it. We proposed solutions for the optimal bandwidth utilization, as well as the per-task joint cost setting and offloading decision from the remote servers, to incentivize offloading while improving their utility. We observed that tasks are computed at different tiers, depending on their payload, and that our solution allocates tasks while avoiding remote infeasibilities. We also observed a tradeoff between costs incurred across tiers where our solution mostly increased the utility at the remote servers while increasing local costs due to offloading of locally infeasible tasks. Future works may tackle the computing resource optimization as well as explicit local infeasibility management.

## ACKNOWLEDGEMENT

This work received funding from Horizon Europe under the Marie Skłodowska Curie actions: ELIXIRION (GA 101120135).

## REFERENCES

- [1] J. Li and P. C. and, "Health care 4.0: A vision for smart and connected health care," *IIE Transactions on Healthcare Systems Engineering*, vol. 11, no. 3, pp. 171–180, 2021. [Online]. Available: <https://doi.org/10.1080/24725579.2021.1884627>
- [2] J. Medina, M. Espinilla, A. García-Fernández, and L. Martínez, "Intelligent multi-dose medication controller for fever: From wearable devices to remote dispensers," *Computers & Electrical Engineering*, vol. 65, pp. 400–412, 2018. [Online]. Available: <https://www.sciencedirect.com/science/article/pii/S004579061730561X>
- [3] Y. Umayahara, Z. Soh, K. Sekikawa, T. Kawae, A. Otsuka, and T. Tsuji, "A mobile cough strength evaluation device using cough sounds," *Sensors*, vol. 18, no. 11, 2018. [Online]. Available: <https://www.mdpi.com/1424-8220/18/11/3810>
- [4] Nick Stockton, "Inside the inflatable hospital that's saving lives in nepal," accessed: 2025-08-28. [Online]. Available: <https://www.wired.com/2015/05/inside-inflatable-hospital-thats-saving-lives-nepal>
- [5] Press and information team of the Delegation to UKRAINE, "12 new modular clinics installed in ukraine in 2024 through who, european union, and ministry of health partnership," accessed: 2025-08-28. [Online]. Available: [https://www.eeas.europa.eu/delegations/ukraine/12-new-modular-clinics-installed-ukraine-2024-through-who-european-union-and-ministry-health\\_en](https://www.eeas.europa.eu/delegations/ukraine/12-new-modular-clinics-installed-ukraine-2024-through-who-european-union-and-ministry-health_en)
- [6] World Economic Forum, "What is a satellite-connected smartphone – and how can it help bridge the digital divide?" October 2022, accessed: 2024-10-16. [Online]. Available: <https://www.weforum.org/agenda/2022/10/satellite-connected-smartphones-digital-divide/>
- [7] Matthew Gover, "Satellite launches soar to record levels in 2025 as new players join the race," accessed: 2025-08-28. [Online]. Available: <https://orbitaltoday.com/2025/06/16/satellite-launches-soar-to-record-levels-in-2025-as-new-players-join-the-race/>
- [8] S. Kumar, J. Krivochiza, T. Yilmaz, J. Querol, S. Chatzinotas, S. Andreacci, and J. Grotz, "5g-nr over transparent payload geo satellites: A hands-on approach using openairinterface5g-ntn," *IEEE Open Journal of the Communications Society*, vol. 6, pp. 5969–5987, 2025.
- [9] GSMA, "High altitude platform systems: Towers in the Skies, version 2.0," GSMA, Tech. Rep., Feb. 2022, white paper. [Online]. Available: <https://www.gsma.com/futurenetworks/wp-content/uploads/2022/02/HAPS-Towers-in-the-skies-draft-v-2.1-clean.pdf>
- [10] X. A. F. Cabezas, K. Ntontin, and S. Chatzinotas, "Adaptive resource initialization for iomt task offloading in ntns," in *IEEE Conference on Network Function Virtualization and Software Defined Networks (NFV-SDN)*. Athens, Greece: IEEE, Nov 2025.
- [11] P. Li, Y. Wang, Z. Wang, T. Wang, and J. Cheng, "Joint task offloading and resource allocation strategy for hybrid mec-enabled leo satellite networks: A hierarchical game approach," *IEEE Transactions on Communications*, vol. 73, no. 5, pp. 3150–3166, 2025.
- [12] G. Im, D. H. Jung, and J. Gyu Ryu, "Enhancing the connectivity of satellite iot devices in terrestrial-non terrestrial integrated networks based on the stackelberg game approach," in *2020 International Conference on Information and Communication Technology Convergence (ICTC)*, 2020, pp. 1783–1785.
- [13] W. Cao, F. Chu, L. Jia, Y. Zhang, and H. Zhou, "Stackelberg game-based anti-jamming channel selection in satellite-terrestrial networks," in *2025 IEEE 101st Vehicular Technology Conference (VTC2025-Spring)*, 2025, pp. 1–5.
- [14] D. Shafaie, J. Hassanpour, A. Karkehabadi, E. Quiñones, and E. Kartasakli, "Competitive task offloading in hierarchical edge-cloud compute continuum," in *IEEE Conference on Network Function Virtualization and Software Defined Networks (NFV-SDN)*. Athens, Greece: IEEE, Nov 2025.
- [15] A. Al-Hourani, S. Kandeepan, and S. Lardner, "Optimal lap altitude for maximum coverage," *IEEE Wireless Communications Letters*, vol. 3, no. 6, pp. 569–572, 2014.
- [16] T. Cheng *et al.*, "IRS-enabled secure G2A communications for UAV system with aerial eavesdropping," *IEEE Sys. J.*, vol. 17, no. 3, pp. 3670–3681, 2023.
- [17] 3GPP, "3rd generation partnership project; technical specification group radio access network; nr; user equipment (ue) radio transmission and reception; part 5: Satellite access radio frequency (rf) and performance requirements (release 18)," 3GPP, Tech. Rep. TS 38.101-5 V18.7.0 (2024-09), 2024.
- [18] 3GPP, "3rd generation partnership project; technical specification group services and system aspects; release 14 description; summary of rel-14 work items (release 14)," 3GPP, Tech. Rep. TR 21.914 V14.0.0 (2018-05), 2018.
- [19] Mario J. Garcia, "Digital echocardiography," accessed: 2025-12-03. [Online]. Available: <https://thoracickey.com/digital-echocardiography/>
- [20] H. Yoo, Y. Yum, S. Park, J. M. Lee, M. Jang, Y. Kim, J.-H. Kim, H.-J. Park, K. S. Han, J. H. Park, and H. J. Joo, "Kurias-ecg: a 12-lead electrocardiogram database with standardized diagnosis ontology (version 1.0)," PhysioNet, 2021, rRID:SCR\_007345.
- [21] P. Cho, J. Kim, B. Bent, and J. Dunn, "Big ideas lab glycemic variability and wearable device data (version 1.1.2)," PhysioNet, 2023, rRID:SCR\_007345.